A Fast HF MLFMA Full-wave Forward Solver for 3-D Lossy Dielectric Objects in a Homogeneous Background

J. De Zaeytijd* A. Franchois† F. Olyslager*

***Abstract* — In this paper we present a fast forward solver for the 3-D volume integral equation (VIE) based on a fast multilevel multipole algorithm (MLFMA). This allows efficient scattering calculations from electrically large inhomogeneous dielectric objects. For some geometries the computational complexity and memory requirements can be as low as $\mathcal{O}(N)$, N being the number of unknowns. In addition we reduce the prefactor using rank revealing QR factorizations (RRQR). The method is a competitive alternative to the conjugate gradient fast Fourier transform (CG-FFT) method in inverse scattering problems.**

1 INTRODUCTION

In this paper we consider the electromagnetic scattering from electrically large inhomogeneous lossy dielectric structures in a homogeneous background. To this end we use the volume integral equation (VIE) and discretize it with a Galerkin method. A classical method of moments (MoM) however is too expensive in computational cost and memory requirements. Even when solved using an iterative Krylov subspace method, the algorithm requires $\mathcal{O}(N^2)$ operations. The conjugate gradient fast Fourier transform method (CG-FFT) [1] is often used to overcome this burden. This algorithm uses a uniform grid with cuboidal cells to model the object and then exploits the Toeplitz property of the interaction matrix by performing the matrix-vector product with a 3-D fast fourier transform (FFT). This reduces the computational complexity to $\mathcal{O}(NlogN)$ and the memory use to $\mathcal{O}(N)$. Still there are some drawbacks to the method.

First of all in CG-FFT the integration over one cell is performed using a simple trapezoidal integration rule, introducing an integration error if the grid is not dense enough. This results in a large number of unknowns. A second drawback is the difficulty to accurately model a curved boundary with cuboidal cells. Both problems can be avoided when using a tetrahedral mesh to model the scatterer.

*INTEC, Ghent University, Sint-Pietersnieuwstraat 41, 9000 Ghent, Belgium, e-mail: jurgen.dezaeytijd@intec.ugent.be

†INTEC-IMEC, Ghent University, Sint-Pietersnieuwstraat 41, 9000 Ghent, Belgium

Several approaches are possible to use the benefits of tetrahedral modeling in combination with a reduced computational complexity. We mention the precorrected FFT method [2], the adaptive integral method (AIM) [3] and finally the multilevel fast multipole algorithm (MLFMA) [4]. The first two methods have the same order of computational complexity and storage requirements as CG-FFT. The MLFMA that constitutes the subject of this paper requires $\mathcal{O}(N)$ operations and memory in case of dense volume scatterers, for example a quasi-equilateral cuboid.

In the following sections we will adress the integral formulation of the scattering problem and some generalities of the MLFMA implementation. Next we will spend some extra attention to a special feature of our approach, namely the use of a rank-revealing QR-factorization (RRQR) [5] to further reduce the costs of the near interactions and the aggregation and disaggregation stages in the algorithm. Finally we will present some numerical examples.

2 FORMULATION

The problem will be formulated in the frequency domain and the time factor $e^{j\omega t}$ will be suppressed.

2.1 Formulation of the VIE

We consider an inhomogeneous dielectric object with complex permittivity $\epsilon(\mathbf{r})$ and permeability μ_0 that is situated in an infinite homogeneous background medium with parameters ϵ_0 and μ_0 which we will denote as free space. The incident electric field $\mathbf{e}^i(\mathbf{r})$ is defined as the field in absence of the object. Using the equivalence principle, we replace the dielectric object by a contrast current distribution in free space

$$\mathbf{J}(\mathbf{r}) = j\omega\frac{\epsilon(\mathbf{r})-\epsilon_0}{\epsilon(\mathbf{r})}\mathbf{d}(\mathbf{r}) = j\omega\chi(\mathbf{r})\mathbf{d}(\mathbf{r}). \quad (1)$$

Here $\mathbf{d}$ is the electric flux density. $\chi(\mathbf{r})$ will be called the contrast function. The contrast charge ρ is given by $\rho = -\frac{1}{j\omega}\nabla\cdot\mathbf{J} = -\nabla\chi\cdot\mathbf{d} - \chi\nabla\cdot\mathbf{d}$. We

now can write down the volume integral equation:

$$\mathbf{e}^i(\mathbf{r}) = \frac{\mathbf{d}(\mathbf{r})}{\epsilon(\mathbf{r})} + \nabla\phi(\mathbf{r}) + j\omega\mathbf{a}(\mathbf{r}), \tag{2}$$

where ϕ and $\mathbf{a}$ are the scalar and vector potential respectively, given by:

$$\mathbf{a}(\mathbf{r}) = j\omega\mu_0 \int G(\mathbf{r}-\mathbf{r}')\chi(\mathbf{r}')\mathbf{d}(\mathbf{r}')\mathrm{d}\mathbf{V}' \tag{3}$$

$$\phi(\mathbf{r}) = -\frac{1}{\epsilon_0}\int G(\mathbf{r}-\mathbf{r}')\nabla'\cdot[\chi(\mathbf{r}')\mathbf{d}(\mathbf{r}')]\mathrm{d}\mathbf{V}' \tag{4}$$

G represents the scalar Green's function

$$G(\mathbf{r}-\mathbf{r}') = \frac{e^{-jk_0|\mathbf{r}-\mathbf{r}'|}}{4\pi \mid \mathbf{r}-\mathbf{r}' \mid} \tag{5}$$

in which $k_0 = \omega\sqrt{\epsilon_0\mu_0}$ is the wavenumber of free space. Equation (2) states that the incident electric field is the difference between the total electric field and the field generated by the contrast currents and charges only, the so-called scattered field.

2.2 Discretization of the VIE

To solve equation (2) for the unknown flux density $\mathbf{d}$ we represent the latter by the Schaubert-Wilson-Glisson basis functions [6] that are associated to the faces of the tetrahedral mesh.

$$\mathbf{d}(\mathbf{r}) = \sum_{n=1}^{N} D_n\mathbf{f}_n(\mathbf{r}) \tag{6}$$

with N the total number of faces in the mesh. Let F_n be an internal face. That means that there are two tetrahedra T_n^+ and T_n^- adjacent to F_n. We define $\mathbf{f}_n^+$ and $\mathbf{f}_n^-$ such that $\mathbf{f}_n(\mathbf{r}) = \mathbf{f}_n^+(\mathbf{r})$ if $\mathbf{r}\in T_n^+$ and $\mathbf{f}_n(\mathbf{r}) = \mathbf{f}_n^-(\mathbf{r})$ if $\mathbf{r}\in T_n^-$. $\mathbf{f}_n(\mathbf{r}) = 0$ elsewhere. If F_n is an external face, then only T_n^+ is defined. The main advantage of these basis functions is that the normal component is continuous across the internal faces so that the boundary condition for $\mathbf{d}$ is fullfilled automatically. We further assume the contrast function to be constant over each tetrahedron ($\chi(\mathbf{r}) = \chi_T$ if $\mathbf{r}\in T$).

By substituting expression (6) into (2) and applying the Galerkin testing procedure, we arrive at a set of N lineair equations that has to be solved.

2.2.1 MLFMA

Since in classical MoM we have to calculate the interactions between each pair of faces, we end up with an $\mathcal{O}(N^2)$ algorithm if we solve the system iteratively. The fast multipole method (FMM) only considers interactions between groups of mesh-elements and reduces the computational cost of the matrix-vector product.

The basis of FMM is formed by the following expansion of the Green's tensor [4]:

$$\bar{\bar{G}}(\mathbf{r}-\mathbf{r}') \approx \frac{-jk_0}{(4\pi)^2}\int \mathrm{d}\hat{k}e^{-j\mathbf{k}\cdot(\mathbf{r}-\mathbf{r}_\lambda)}T_{\lambda\lambda'}(\hat{k})(\bar{\bar{I}}-\hat{k}\hat{k})e^{j\mathbf{k}\cdot(\mathbf{r}'-\mathbf{r}_{\lambda'})} \tag{7}$$

where $\mathbf{k} = k_0\hat{k}$ and where

$$T_{\lambda\lambda'}(\hat{k}) = \sum_{l=0}^{L}(-j)^l(2l+1)h_l^{(2)}(k_0r_{\lambda\lambda'})P_l(\hat{k}\cdot\hat{r}_{\lambda\lambda'}) \tag{8}$$

is called the translation operator. $h_l^{(2)}$ is the spherical Hankel function of the second kind, P_l is the Legendre function of order l and $\mathbf{r}_{\lambda\lambda'} = \mathbf{r}_\lambda - \mathbf{r}_{\lambda'}$. In addition $r_{\lambda\lambda'} > d$ with $\mathbf{d} = (\mathbf{r}-\mathbf{r}_\lambda) - (\mathbf{r}'-\mathbf{r}_{\lambda'})$. Using (7) we can write down the scattered field due to the current in T and weighted over T_m^+:

$$\int_{T_m^+}\mathbf{f}_m^+\cdot\mathbf{e}_T^s\mathrm{d}V = \frac{k_0^2}{\epsilon_0}\sum_{n\in\alpha_T}D_n\chi_T\int_{T_m^+}\mathrm{d}V\mathbf{f}_m^+(\mathbf{r})\cdot\int_T\mathrm{d}V'\bar{\bar{G}}(\mathbf{r}-\mathbf{r}')\cdot\mathbf{f}_n^\pm(\mathbf{r}') = \frac{-jk_0}{(4\pi)^2}\int\mathrm{d}\hat{k}\mathbf{D}_{T_m^+,\lambda}(\hat{k})\cdot T_{\lambda\lambda'}(\hat{k})\mathbf{U}_{T,\lambda'}(\hat{k}) \tag{9}$$

α_T contains the numbers of the faces of T and

$$\mathbf{U}_{T,\lambda'} = \frac{k_0^2}{\epsilon_0}\chi_T\sum_{n\in\alpha_T}D_n\int_T e^{j\mathbf{k}\cdot(\mathbf{r}'-\mathbf{r}_{\lambda'})}(\bar{\bar{I}}-\hat{k}\hat{k})\mathbf{f}_n^\pm\mathrm{d}V' \tag{10}$$

$$\mathbf{D}_{T_m^+,\lambda} = \int_{T_m^+}e^{-j\mathbf{k}\cdot(\mathbf{r}-\mathbf{r}_\lambda)}\mathbf{f}_m^+\mathrm{d}V \tag{11}$$

and a similar expression if weighted over T_m^-. In equations (9) and (10) the $\pm$-sign should be replaced by $+$ if $T = T_n^+$ and by $-$ if $T = T_n^-$. From (9) the principle of FMM can be seen. First we divide the mesh elements into groups, for example group $G_{\lambda'}$, centered around $\mathbf{r}_{\lambda'}$. We then calculate the radiation pattern $\mathbf{U}_{\lambda'}$ of $G_{\lambda'}$ by summing the radiation patterns $\mathbf{U}_{T,\lambda'}$ for all $T\in G_{\lambda'}$. This involves only single integrals. We then shift this pattern by multiplication with $T_{\lambda\lambda'}$ to the center $\mathbf{r}_\lambda$ of G_λ where it is projected onto the basisfunctions by $\mathbf{D}_{T_m^\pm,\lambda}$. The radiation patterns turn out to be quasi band limited, which allows us to recontstruct them using only a minimal amount of samples. If this procedure is repeated for every pair of groups, the number of operations is reduced compared to the calculation of every interaction between pairs of basis functions.

Unfortunately the accuracy of the expansion (7) breaks down when L grows too large. This is due to a numerical instability when l exceeds the argument of $h_l^{(2)}$. For nearby groups this happens before the summation in (8) has converged to the desired accuracy. This means that we still have to calculate some interactions following the classical MoM-scheme, the so-called near interactions. We call the groups for which we can use the expansion *well-separated*.

The FMM can be extended to a multilevel algorithm resulting in the MLFMA [4] which yields a $\mathcal{O}(N)$ computational complexity and memory use in case of dense volume scatterers.

2.2.2 Use of RRQR

The number of samples, needed for an accurate representation of the radiation pattern of a group is proportional to its surface area and the number of unknowns in the group is proportional to its volume. This means a reduction of the information used to calculate the interactions between well-separated groups. Even for nearby groups, which are still treated in the classical way, we can eliminate some information.

Suppose A is the $(m \times n)$-matrix that contains the interactions between two nearby (but not coinciding) groups. It turns out that this matrix is rank-deficient if the groups contain a lot of mesh elements, which is the case in dense volume scatterers. We can calculate a rank-revealing QR (RRQR) factorisation of this matrix:

$$A = QRP^T \tag{12}$$

where Q is a unitary matrix, R is upper triangular and P is a permutation matrix. Since A is rank deficient we can define a numerical rank $k < min(m, n)$ with respect to a given threshold τ. This means that $\sigma_{k+1}(A)/\sigma_1(A) < \tau$, where $\sigma_i(A)$ is the ith singular value of A.

We now truncate the RRQR-factorization, i.e. replace Q and R by Q', which only contains the first k columns of Q, and R', which is formed by the first k rows of R. Now we have an approximation $A' = Q'R'P^T$ to the matrix A. The algorithm we use to calculate the RRQR-factorization [5] guarantees that $\|A - A'\|_2 \leq \rho\sigma_{k+1}(A)$, where ρ depends on k and n. With this we get $\|A - A'\|_2/\|A\|_2 \leq \rho\sigma_{k+1}(A)/\sigma_1(A) < \rho\tau$. So the error on the matrix approximation is controllable.

How does this relate to the relative error on the product of A with a n-dimensional vector x? This is not a simple question. We only give some qualitative remarks and some numerical examples. Truncating a rank revealing factorization of a rank-deficient A actually means the replacement of the numerical null-space $N(A)$ of A by an exact null-space $N'(A')$. We write x as $x = x_0 + x_1$ where x_0 belongs to $N(A)$ (and $N'(A')$) and x_1 does not. We then get

$$\frac{\|Ax - A'x\|_2}{\|Ax\|_2} = \frac{\|Ax_0\|_2}{\|Ax_1 + Ax_0\|_2}. \tag{13}$$

Since $x_1 \notin N(A)$ the term Ax_1 will dominate the denominator of (13) and the relative error on $A'x$ will be small. However, when $x_1 = 0$ it can become as large as one. The fact that this doesn't generate problems in the matrix-vector product with the complete interactionmatrix can be explained as follows. When a factorized block A of the matrix gets multiplied by a vector from $N(A)$, this product will only marginally contribute to the total matrix-vector product just because the vector belongs to $N(A)$.

The advantage of the truncated factorization of near-intaraction matrices is dual: it reduces memory use and speeds up the matrix-vector multiplication Ax. The gain in both cases is given by $(mn)/(k(m+n))$.

Besides the near-interactions we also use the RRQR-factorization on the aggregation and disaggregation step. Aggregation is calculating the radiation pattern of a group from the expansion coefficients D_n of basisfunctions that lie in that group and disaggregation is the projection of the shifted pattern onto the basisfunctions. Tables 1 and 2 give some numerical examples.

τ	solution	agg.	disagg.
$1e-5$	$2.7399e-5$	$1.3189e-4$	$7.5793e-5$
$1e-6$	$6.7823e-6$	$1.2482e-5$	$1.7309e-5$
$1e-7$	$1.6903e-6$	$1.0898e-6$	$1.0898e-6$

Table 1: Relative errors on solution, aggregation matrix and disaggregation matrix for different τ in a configuration with two well-separated cubic groups, each with side $0.3\lambda_0$ and containing 324 faces.

τ	solution	near-interaction matrix
$1e-5$	$4.5543e-6$	$1.5211e-04$
$1e-6$	$4.5481e-7$	$9.1140e-06$
$1e-7$	$6.0865e-8$	$1.5039e-06$

Table 2: Relative errors on solution and near-interaction matrix for different τ in a configuration with two nearby cubic groups, each with side $0.4\lambda_0$ and containing 736 faces.

3 NUMERICAL EXAMPLES

First of all we illustrate the correctness of our MoM-discretization of the VIE. To this end we calculated the scattered field for a homogeneous sphere with radius $a = \lambda_0/10$ at a distance $d = \lambda_0/2$ from the center of the sphere. λ_0 is the wavelength in free space. The sphere has permittivity $\epsilon = 5\epsilon_0$. The incident field is linearly polarised along the x- axis with amplitude $E_0 = 1$ and propagates along the positive z -axis. We compare the numerical solution to the analytic solution given by the Mie series. The mesh used for this problem consisted of 1088 faces. The result is shown in figure 1.

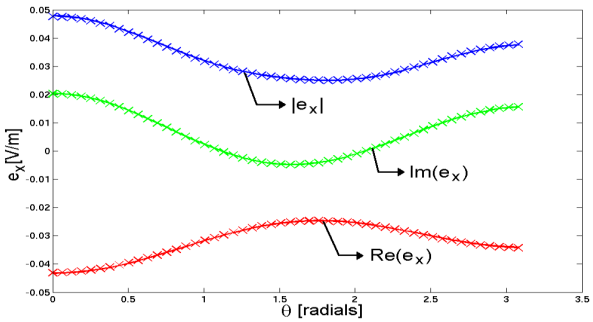

Figure 1: e_x plotted for $\phi = \pi/4$ and for $\theta \in [0, \pi]$. The solid line is the Mie-series solution and the numerical solution is represented by $\times$.

Finally we present the time for one matrix-vector multiplication versus the number of unknowns in figure 2. The testing geometry consists of a cuboidal object that has dimensions $\lambda_0 \times \lambda_0 \times l$ where l varies from $2\lambda_0$ to $18\lambda_0$ in order to change the number of unknowns N. Since the geometry is altered just in one direction, thus is not a dense volume scatterer, the computational complexity is actually not assymptotically of $\mathcal{O}(N)$, but we do notice a cross-over point. Also the effect of the RRQR is illustrated. The reason that we present this example and not a dense volume scatterer is that our implementation still has to be further optimized, especially in memory management. But we are confident that we will be able to do so in the near future.

4 CONCLUSIONS

We have solved the VIE by discretising it with tetrahedral meshes and using the MLFMA. Compared to the CG-FFT this has the advantages of an accurate and more flexible way of modeling the inhomogeneous object with less unknowns. Moreover it reduces the computational complexity from $\mathcal{O}(NlogN)$ to $\mathcal{O}(N)$ in case of dense volume scatterers, which is especially usefull for electrically very large problems.

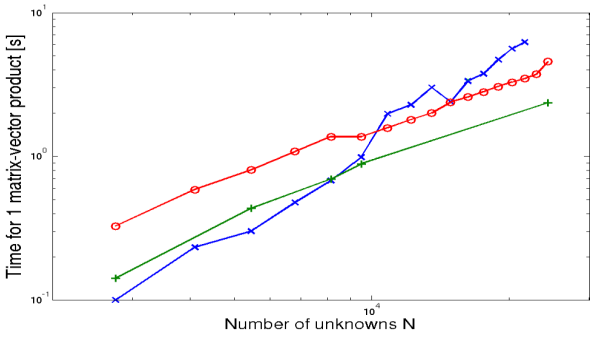

Figure 2: Time for matrix-vector product versus number of unknowns. $\times$ represents the classical MoM calculation and $\circ$ the MLFMA. The $+$-curve is calculated with application of RRQR ($\tau = 1e{-}5$).

Acknowledgments

Jürgen De Zaeytijd is a Research Assistant of the Fund for Scientific Research - Flanders (F.W.O. - Vlaanderen).

References

[1] T.K. Sarkar, E. Arvas and S.M. Rao, "Application of FFT and the conjugate gradient method for the solution of electromagnetic radiation from electrically large and small conducting bodies", IEEE Trans. Antennas Propag., vol. 34, no. 5, pp. 635-640, May 1986.

[2] X. Nie, L. Lie, N. Yuan, T.S. Yeo and Y. Gan, "Precorrected-FFT solution of the volume integral equation for 3-D inhomogeneous dielectric objects", IEEE Trans. Antennas Propag., vol. 53, no. 1, pp. 313-319, January 2005.

[3] Z.Q. Zhang and Q.H. Liu, "A volume adaptive integral method (VAIM) for 3-D inhomogeneous objects", IEEE AntennasWireless Propag. Lett., vol. 1, pp. 102-105, Jul. 2002.

[4] W. Chew, J. Jin, E. Michielssen and J. Song, "Fast and effiecient algorithms in computational electromagnetics", Artech House, 2001.

[5] C.H. Bischof and G. Quintana-Ort, "Computing Rank-Revealing QR Factorizations of Dense Matrices". ACM Trans. Math. Softw., vol. 24, no.2, pp. 226-253, 1998.

[6] D.H. Schaubert, D.R. Wilton and A.W. Glisson, "A tetrahedral modeling method for electromagnetic scattering by arbitrarily shaped inhomogeneous dielectric bodies", IEEE Trans. Antennas Propag., vol. 32, no. 1, January 1984.

Session 12: INVERSE SCATTERING AND REMOTE SENSING

Session 13: INTEGRAL EQUATION METHODS: Part 2

PROCEEDINGS
OF JOINT

9th International Conference on Electromagnetics in Advanced Applications ICEAA '05

and

11th European Electromagnetic Structures Conference EESC '05

Under the auspices of and supported by

CITTA' DI TORINO

ICEAA '05 - 9th International Conference on Electromagnetics in Advanced Applications and EESC '05 - 11th European Electromagnetic Structures Conference

September 12-16, 2005

Torino, Italy

ISBN 88-8202-093-2